Journal of Applied Pharmaceutical Science Vol. 0(00), pp 001-012, 2024
Available online at http://www.japsonline.com
DOI: 10.7324/JAPS.2024.161007
ISSN 2231-3354

Dipeptidyl peptidase-4 inhibition of *Peronema canescens* Jack leaves and stems: Bioassay-guided fractionation, compound profiling by LC-MS/MS, and interaction mechanism

Berna Elya[1], Roshamur Cahyan Forestrania[1], Najihah Mohd Hashim[2,4], Nita Triadisti[1,3]*

[1]Faculty of Pharmacy, Universitas Indonesia, 16424, Depok, Indonesia.
[2]Department of Pharmaceutical Chemistry, Faculty of Pharmacy, Universiti Malaya, 50603 Kuala Lumpur, Malaysia.
[3]Faculty of Pharmacy, Universitas Muhammadiyah Banjarmasin, 70115, Banjarmasin, Indonesia.
[4]Centre for Natural Products Research and Drug Discovery (CENAR), Universiti Malaya, 50603, Kuala Lumpur, Malaysia.

ARTICLE HISTORY
Received on: 13/07/2023
Accepted on: 01/11/2023
Available Online: XX

Key words:
Peronema canescens Jack, dipeptidyl peptidase-4 (DPP-4), bioassay-guided fractionation, UPLC-ESI-QToF-MS/MS, compound profiling.

ABSTRACT

Sungkai (*Peronema canescens* Jack) has been used for generations as a traditional antidiabetic drug for the Borneo people, but scientific data as a dipeptidyl peptidase-4 (DPP-4) inhibitor has never been reported. This study aims to obtain the most active chromatographic fraction as a DPP-4 inhibitor and the profile of the compounds contained. Bioassay-guided fractionation was used in this study and bioassays using spectrofluorometric principles. Compound profiling is carried out using ultra-performance liquid chromatography coupled with electrospray ionization/quadrupole-time-of-flight mass spectrometry (UPLC-ESI-QToF-MS/MS), and molecular docking is used to investigate interactions between compounds and DPP-4. The study found that the most effective extracts were ethyl acetate and methanol extracts from the leaves, which showed inhibitory percentages of 70.0% ± 0.7233% and 59.69% ± 1.9394%, respectively, at a concentration of 100 µg/ml. The fractionation produces the most active fraction, the second fraction from *P. canescens* methanol extract (FPSM2 fraction), with a percent inhibition of 88.28% ± 2.1204%. The compounds contained in FPSM2 were identified through UPLC-ESI-QToF-MS/MS, including pectolinarigenin, glycitein, formononetin, latifoline, 3-oxo-alpha-ionol, moracin M, and loliolide. Assay results showed that *P. canescens* has been shown to have inhibitory activity against DPP-4, suggesting that this plant has excellent potential to be developed as a DPP-4 inhibitor.

INTRODUCTION

Diabetes mellitus is a chronic metabolic health problem with the main characteristic of persistent hyperglycemia. This health disorder causes death and disability throughout the world and attacks the health of many people regardless of gender, age, or country [1–3]. Type 2 diabetes is the most common type of diabetes, accounting for more than 90% of all diabetes cases worldwide. In type 2 diabetes, hyperglycemia is initially a result of the body's cells being unable to respond optimally to insulin, and this condition is called insulin resistance. With the emergence of insulin resistance, the hormone becomes less effective and encourages increased insulin production so that, ultimately, insulin production is no longer adequate. This occurs due to the failure of pancreatic beta cells to produce insulin [4]. The pathophysiology of type 2 diabetes mellitus is related to insulin resistance and insulin secretion, which results in abnormally high blood glucose levels. In cases of cell dysfunction, there is a lack of insulin secretion, thereby limiting the body's capacity to maintain physiological glucose levels. Insulin receptors also contribute to increased glucose production in the liver and decreased glucose uptake in muscle, liver, and adipose tissue [5]. The global incidence of diabetes has continued to increase for several decades, and currently, around 537 million cases of diabetes have been reported. This case continues to expand and is estimated to reach 643 million in 2030 [4,6]. Different treatment

*Corresponding Author
Nita Triadisti, Faculty of Pharmacy, Universitas Muhammadiyah Banjarmasin, 70115, Banjarmasin, Indonesia.
E-mail: triadisti @ gmail.com

classes for type 2 diabetes have shown treatment benefits, but incidence continues to increase, encouraging new agent therapy discoveries to treat type 2 diabetes [7].

Currently, dipeptidyl peptidase-4 (DPP-4) inhibitors are used to treat type 2 diabetes mellitus, and this enzyme is one of the active ingredients in treating type 2 diabetes mellitus. DPP-4 promotes the breakdown of the incretin hormones glucagon-like peptide-1 and glucose insulinotropic peptide by dispensing with the N-terminal dipeptide in the form of the hormone [8,9]. Inhibition of DPP-4 protects glucagon-like peptide-1 and glucose insulinotropic peptide from degradation, thereby increasing insulin secretion to help lower blood sugar levels [10]. DPP-4 inhibitors do not cause weight gain, hypoglycemia, or indigestion and can be administered to patients with renal impairment. They are one of the first-line therapies in managing diabetes [11]. Although most synthetic DPP-4 inhibitors are broadly well-tolerated, some side effects have been reported lately, including headaches, nasopharyngitis, and urinary infections [12]. Hence, it is necessary to identify DPP-4 inhibitors from natural products and explore their activity for diabetes mellitus therapy development [13].

One of the potential Borneo medicinal plants is Sungkai (*Peronema canescens* Jack). This plant has been used for generations as a traditional antidiabetic drug for the Borneo people. The activity of *P. canescens* fractions as an antidiabetic has never been reported, including scientific data on this plant as a DPP-4 inhibitor. The scientific data related to the antidiabetic activity of Sungkai is an *in vivo* study [14] that significantly reduces blood sugar levels. With its popular use as an empirical antidiabetic, there is preliminary data about the potential of this plant in lowering blood sugar levels. Still, there is no scientific data on *P. canescens* as a DPP-4 inhibitor, encouraging research to reveal the activity of this plant as a DPP-4 inhibitor.

In this study, the leaves and stems of *P. canescens* were extracted by three-graded maceration using n-hexane, ethyl acetate, and methanol as solvents, and each extract was investigated for its inhibitory activity against the enzyme DPP-4. Next, the best extracts in DPP-4 inhibition were fractionated using column chromatography. Fractionation using this method is expected to be able to separate the active part of the extract, so the chromatographic fractions will generally have better activity than the original extract [15]. Compound profiling using ultra-performance liquid chromatography coupled with electrospray ionization/ quadrupole-time-of-flight mass spectrometry (UPLC-ESI-QToF-MS/MS) is performed on the most active chromatographic fraction to reveal the compounds contained therein. The interaction between these compounds and DPP-4 will be revealed through molecular docking.

MATERIALS AND METHODS

Plant material

Peronema canescens was collected from Tabalong, South Borneo, Indonesia, during the dry season. The cleaned fresh plant, leaves (5 kg), and stems (3 kg) were dried in an oven at 40°C. The dried leaves and stems are pulverized separately with a grinder, yielding 1.2 kg powdered leaves (24% yield) and 1.1 kg powdered stems (36.67% yield), then refrigerated at 8°C while pending analysis. Plant authenticity was determined, and a voucher specimen was deposited in the faculty of pharmacy, Universitas Indonesia (voucher specimen number 208a/LB/XI/2022).

Chemicals and instrumentation

Chemicals: DPP-4 inhibitor screening assay kit (Cayman Chemicals, Catalog no.700210), analytical and distilled technical grade n-hexane, ethyl acetate, and methanol (Smartlab), Silica Gel 70-230 mesh (Merck), and thin-layer chromatography plate Silica Gel 60 F_{254} (Merck). Instrumentations: Rotary evaporator (IKA), UV lamp (Camag), Microplate reader (Glomax Promega), UPLC-ESI-QToF-MS/MS (Acquity UPLC H-Class System, Waters USA; Xevo G2-S QToF, Waters USA).

Extraction

Peronema canescens leaves (1.2 kg) were extracted by three-graded maceration using n-hexane, ethyl acetate, and methanol as solvents (1:20). By increasing the polarity of the solvent, extracts with different polarities were obtained. Maceration was performed twice for each solvent, with the filtrate being concentrated on a rotary evaporator and the solvent removed. Extraction by this method produced n-hexane extract, ethyl acetate extract, and methanol extract from *P. canescens* leaves. The stems (1.1 kg) were also extracted using the same procedure as the leaves.

Fractionation

Fractionation was performed on selected extracts showing the best activity in inhibiting DPP-4, namely ethyl acetate and methanol extract from the leaves of *P. canescens*. Fractionation using the column chromatography method with a column length of 50 cm and a diameter of 3.5 cm. A gradient system is applied to this fractionation using a combination of eluents starting with n-hexane-ethyl acetate (9:1, 8:2, and up) to the eluent ethyl acetate-methanol (10:0, 9:1, 8:2, and so on until methanol 100%). Elution results were collected every 100 ml and analyzed for chromatogram patterns using thin-layer chromatography.

DPP-4 inhibition activity

The inhibitory activity of DPP-4 was performed on all extracts and chromatographic fractions of *P. canescens* using the test protocol specified by the manufacturer [16]. This assay uses sitagliptin as the standard inhibitor of DPP-4 and Gly-Pro-7-Amido-4-methylcoumarin as the substrate. Briefly, this assay has the principle that DPP-4 decomposes the substrate into fluorescent products, namely the free amido-4-methyl coumarin group, which measures its fluorescence with an excitation wavelength of 350–360 and an emission wavelength of 450–465 using a microplate reader (Glomax Discover System). Fluorescence data were obtained by triplication with the calculation of percent inhibition using the following formula determined by the manufacturer.

Compound profiling using UPLC-ESI-QToF-MS/MS

Compound profiling was performed using UPLC (Acquity UPLC®, Waters, USA) and mass spectrometer

(Xevo G2-S QToF, Waters, USA). Liquid chromatography separation using a C18 column (Acquity UPLC®, Waters, USA) at column temperature 50°C and room temperature 25°C. The eluent consists of 5 mM ammonium formic water and acetonitrile with 0.05% formic acid using a flow rate of 0.2 ml/minute (step gradient). The mass spectrometry was performed using electrospray ionization (positive mode) and quadrupole time-of-flight (QToF) mass analyzer. The electrospray interface system connected the UPLC separation output system to the mass spectrometer. Compound profiling with the mass spectrometer using conditions: the collision energy 4 Ev (low energy) and high energy collision varied between 25 and 60 V. Cone and desolvation gas flow 0 and 793 l/hour were also used correspondingly, source temperature 100°C and desolvation temperature 350°C. Data acquisition and analysis were processed with Masslynx software.

Molecular docking

The 3-D structures of the compounds glycitein (5317750), pectolinarigenin (5320438), formononetin (5280378), latifoline (5281736), moracin M (185848), loliolide (100332), 3-oxo-alpha-ionol (5370052), and sitagliptin (4369359) were downloaded from the PubChem NCBI database. The 3-D structure of the target protein, DPP-4, was downloaded from the Protein Data Bank database with access code 3G0B [17]. The ligands structure (sitagliptin as a commercial drug, and 2-({6-[(3R)-3-aminopiperidin-1-yl]-3-methyl-2,4-dioxo-3,4-dihydropyrimidin-1(2H)-yl}methyl)benzonitrile as a native ligand) were carried out from the PubChem NCBI database as sdf file (3-D form).

Table 1. Extracts yield with various solvents.

Plant sample	Solvent	Simplisia weight	Extract weight	% Yield
Leaves	n-hexane	1.2 kg	18.78 g	1.57%
	ethyl acetate		64.32 g	5.36%
	methanol		86.32 g	7.19%
Stems	n-hexane	1.1 kg	16.42 g	1.49%
	ethyl acetate		52.41 g	4.76%
	methanol		78.36 g	7.12%

Table 2. DPP-4 inhibition on various extracts of *P. canescens* at 100 µg/ml.

Plant sample	Solvent	Percent inhibition (%)			Percent inhibition (%) ± SD
		Data 1	Data 2	Data 3	
Leaves	n-hexane	17.53	16.97	17.36	17.29 ± 0.2898
	ethyl acetate	70.93	69.66	69.68	70.09 ± 0.7233
	methanol	59.59	61.68	57.80	59.69 ± 1.9394
Stems	n-hexane	31.22	30.28	31.80	31.10 ± 0.7675
	ethyl acetate	59.78	56.62	59.78	58.20 ± 1.8244
	methanol	51.27	42.15	45.63	46.35 ± 4.5989

Data are mean ± SD or Percent Inhibition (%) ± SD for triplicate measurements.

Both compounds and targeted protein were imported to the Molegro virtual docker version 5.0. The Molegro virtual Docker 5.0 program predicted the protein structure in the cavities with a maximum molecular surface van der Waals as a parameter [18]. The active side of DPP-4 protein was on the protein grid X = 44.79 A; Y = 32.64 A; Z = 18.74 A; radius 11. Those protein grids were used for ligands-protein docking [18]. Docking parameters with Molegro virtual docker are Score Function Moldock Score [Grid]; grid resolution 0.30; algorithm MolDock SE; the number of runs 10, max iteration 1,500; max population size 50; pose generation energy threshold 100, tries 10–30; simplex evolution max steps 300; neighbor distance factor 1.00; multiple poses the number of poses 5; energy threshold 0.00; and cluster similar poses Root Mean Square Deviation (RMSD) threshold 1. Docking data were visualized with the PyMol 2.3 and the Discovery Studio version 21.1.1. Interaction analysis was performed with the Discovery Studio program version 21.1.1.

RESULT

Extraction and DPP-4 inhibition activity of extracts

The extraction was performed on the leaves and stems of *P. canescens*. Each part of the plant was macerated using a solvent of the increasing polarity of n-hexane, ethyl acetate, and methanol. The yield of the obtained extract is shown in Table 1, and each extract's activity is shown in Table 2.

Fractionation and DPP-4 inhibition activity of fractions

Two extracts with the best inhibitory activity, ethyl acetate and methanol extract from the *P. canescens* leaves, were further fractionated using column chromatography with a silica gel stationary phase and a gradient system with different solvents to generate increased polarity. The results of the fractionation of ethyl acetate and methanol extract of the leaves part are shown in Tables 3 and 4, which show the eluent

Table 3. Eluent and mass of ethyl acetate fractions from *P. canescens* leaves.

Fraction	Eluent of column	Mass of fraction (mg)
FPSEA1	n-Hxn/Ea = 9: 1	473
FPSEA2	n-Hxn/Ea = 8: 2	306
FPSEA3	n-Hxn/Ea = 8: 2	217
FPSEA4	n-Hxn/Ea = 7: 3	440
FPSEA5	n-Hxn/Ea = 6: 4–5: 5	1,593
FPSEA6	n-Hxn/Ea = 4: 6–3: 7	1,969
FPSEA7	n-Hxn/Ea = 2: 8–1: 9	551
FPSEA8	n-Hxn/Ea = 1: 9–0: 10	816
FPSEA9	n-Hxn/Ea = 0: 10	808
FPSEA10	Ea/Met = 9: 1–8: 2	879
FPSEA11	Ea/Met = 7: 3–2: 8	443
FPSEA12	Ea/Met = 1: 9–0: 10	1,171

Description: FPSEA: fraction from ethyl acetate extract, n-Hxn = n-Hexane, Ea = ethyl acetate, Met = methanol.

Table 4. Eluent and mass of methanol fractions from *P. canescens* leaves.

Fraction	Eluent of column	Mass of fraction (mg)
FPSM1	n-Hxn/Ea = 8: 2	65
FPSM2	n-Hxn/Ea = 7: 3–6: 4	202
FPSM3	n-Hxn/Ea = 5: 5	141
FPSM4	n-Hxn/Ea = 4: 6–3: 7	236
FPSM5	n-Hxn/Ea = 2: 8–1: 9	61
FPSM6	n-Hxn/Ea = 0: 10	1,053
FPSM7	n-Hxn/Ea = 0: 10–Ea/Met = 9: 1	4,890
FPSM8	Ea/Met = 8:2	1,826
FPSM9	Ea/Met = 7: 3–1: 9	1,048
FPSM10	Ea/Met = 0: 10	1,504

Description: FPSM: fraction from methanol extract, n-Hxn = n-Hexane, Ea = ethyl acetate, Met = methanol.

of each fraction so that the polarity conditions of each fraction can be described and the mass of each fraction obtained. The fractions were then assayed for inhibitory activity against DPP-4, and the results are shown in Tables 5 and 6. The assay results showed that all fractions had inhibitory activity against DPP-4.

Compound profiling of the most active fraction in DPP-4 inhibition

The identification of the compounds in FPSM2 as the most active fraction was done by UPLC-QToF-MS/MS. The Masslynx software processed the data obtained, giving an overview of the compounds contained in FPSM2. The chromatogram of FPSM2 using UPLC-QToF-MS/MS is shown in Figure 1. Table 7 presents UPLC-MS/MS analysis

Table 5. Percent inhibition of ethyl acetate extract's fractions against DPP-4.

Sample (100 µg/ml)	Percent inhibition (%)			Mean ± SD
	Data 1	Data 2	Data 3	
FPSEA1	18.05	28.28	21.96	22.76 ± 5.1621
FPSEA2	19.75	22.22	17.60	19.86 ± 2.3118
FPSEA3	82.30	83.11	81.99	82.47 ± 0.5783
FPSEA4	75.43	75.33	74.97	75.24 ± 0.2419
FPSEA5	71.62	65.[illegible]	71.39	69.54 ± 3.3997
FPSEA6	34.44	37.73	38.67	36.94 ± 2.2211
FPSEA7	56.21	56.75	55.77	55.91 ± 0.2600
FPSEA8	76.10	77.91	78.53	77.51 ± 1.2626
FPSEA9	72.40	73.09	72.11	72.54 ± 0.5034
FPSEA10	77.38	78.37	77.32	77.69 ± 0.5897
FPSEA11	56.11	58.32	57.92	57.48 ± 1.1776
FPSEA12	30.16	29.67	27.22	29.18 ± 1.5751
Sitagliptin	96.25	96.25	96.43	96.31 ± 0.1096

Data are mean ± SD or Percent Inhibition (%) ± SD for triplicate measurements.

Table 6. Percent inhibition of methanol extract's fractions against DPP-4.

Sample (100 µg/ml)	Percent inhibition (%)			Mean ± SD
	Data 1	Data 2	Data 3	
FPSM1	19.03	15.26	13.10	15.80 ± 3.0020
FPSM2	89.40	85.83	89.60	88.28 ± 2.1204
FPSM3	85.53	85.53	85.39	85.49 ± 0.0854
FPSM4	65.25	65.18	65.31	65.25 ± 0.0629
FPSM5	63.34	65.55	65.98	64.95 ± 1.4155
FPSM6	69.45	69.55	68.40	69.13 ± 0.6387
FPSM7	73.81	74.75	73.41	73.99 ± 0.6882
FPSM8	57.67	58.97	53.06	56.57 ± 3.1098
FPSM9	81.33	80.15	70.01	77.17 ± 6.2221
FPSM10	56.88	59.25	63.38	59.84 ± 3.2914
Sitagliptin	96.25	96.25	96.43	96.31 ± 0.1096

Data are mean ± SD or Percent Inhibition (%) ± SD for triplicate measurements.

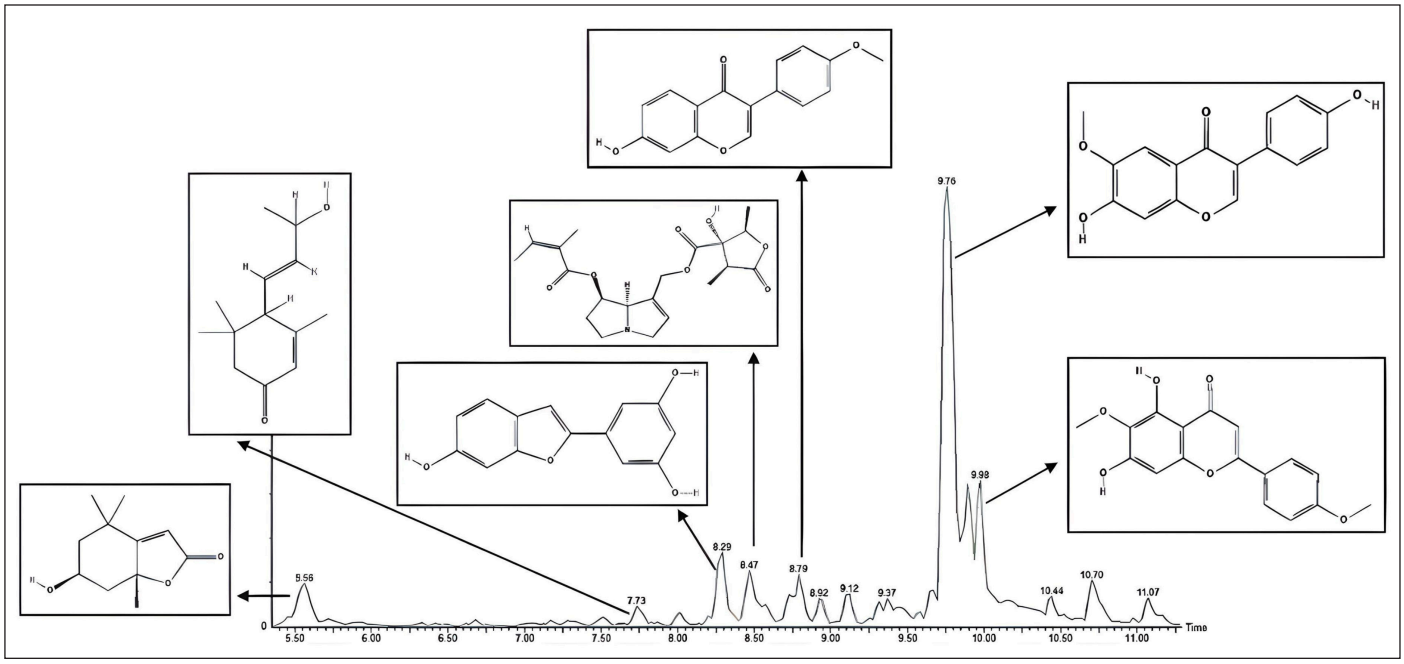

Figure 1. The chromatogram of FPSM2.

Table 7. Compounds identified in the most active fraction (FPSM2) from *P. canescens* leaves.

No	Retention time (minute)	$[M+H]^+$, *m/z*	Ion fragments, *m/z*	Formula, $[M+H]^+$	Compound
1	9.98	315.0872	271.0612 299.1647	$C_{17}H_{15}O_6$	Pectolinarigeni 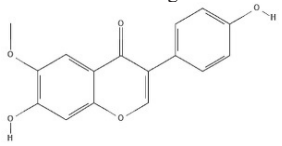
2	9.76	285.0777	242.0589 124.0172 270.0537 167.0356	$C_{16}H_{13}O_5$	Glycitein 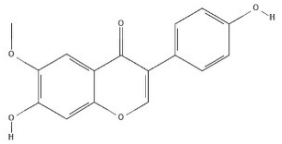
3	8.79	269.0816	137.1034 239.1031 241.1234 243.1337	$C_{16}H_{13}O_4$	Formononetin 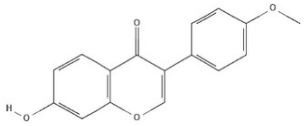
4	8.47	394.1875	131.0869 159.1185 189.1296 383.1487	$C_{20}H_{28}NO_7$	Latifoline 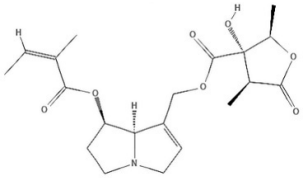

(Continued)

No	Retention time (minute)	$[M+H]^+$, *m*/*z*	Ion fragments, *m*/*z*	Formula, $[M+H]^+$	Compound
5	8.29	243.0671	111.0786 133.1059 213.1252 225.1299	$C_{14}H_{11}O_4$	Moracin M 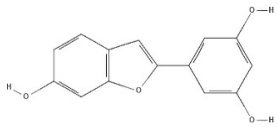
6	7.73	209.1548	151.0728 165.0638 173.1360 191.1430	$C_9H_{17}N_6$	3-oxo-α-ionol 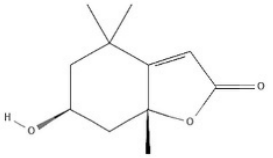
7	5.56	197.1185	81.0730 135.1206 137.1064 153.0856	$C_{11}H_{17}O_3$	Loliolide 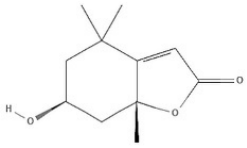

results, including retention time (rt), precursor ion mass (*m*/*z*, positive mode), ion fragments formed, and the formula of each compound.

Molecular docking

The compounds detected in the profiling on the most active fraction were investigated for the mechanism of interaction with the DPP-4 enzyme protein using molecular docking. Visualization of the interaction between these compounds and the DPP-4 enzyme can be seen in Figures 3–5. The interactions' details, including binding energy, binding category, and binding type, as well as the amino acid residues that interact, can be seen in Table 8.

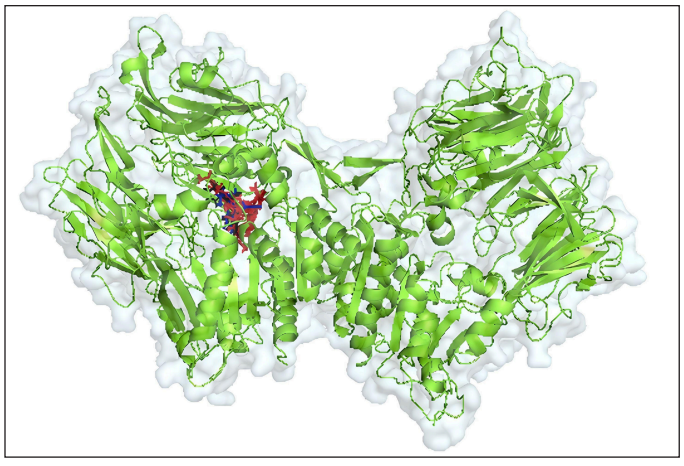

Figure 2. 3-D structure of the compound-complex with DPP-4 protein, red shows the target compound, blue shows the compound structure of sitagliptin (control), and black shows the compound 2-({6-[(3R)-3- aminopiperidin-1-yl]-3-methyl-2,4-dioxo-3,4-dihydropyrimidin-1(2H)-yl}methyl)benzonitrile, while green is the DPP4 protein.

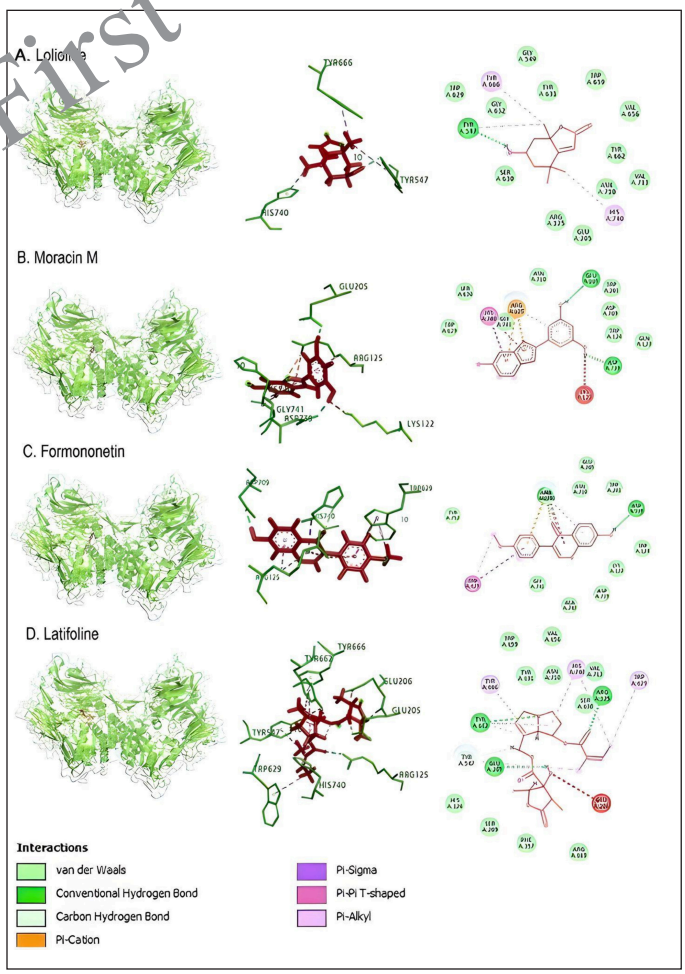

Figure 3. In the interaction between loliolide, moracin M, formononetin, and latifoline compounds with DPP4 protein, red indicates the target compound, while green is the DPP-4 protein.

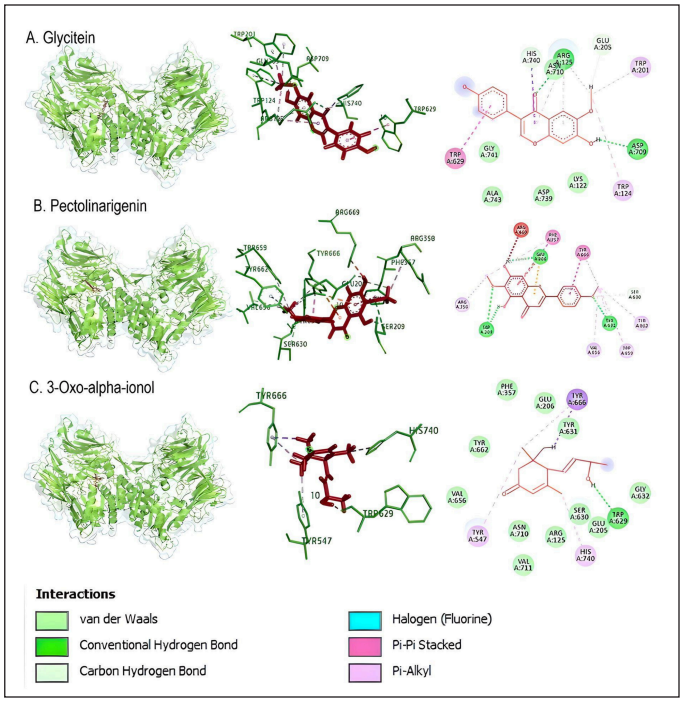

Figure 4. Interaction of glycitein, pectolinarigenin, and 3-oxo-alpha-ionol compounds with DPP-4 protein.

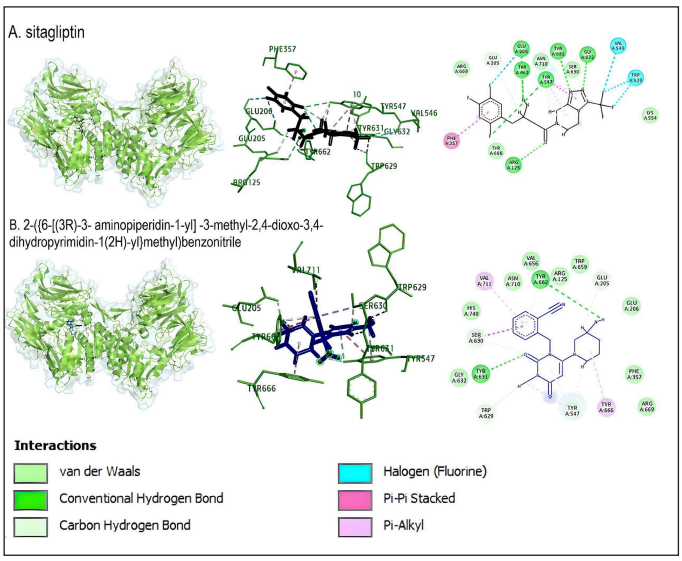

Figure 5. Interaction of sitagliptin and 2-({6-[(3R)-3-aminopiperidin-1-yl]-3-methyl-2,4-dioxo-3,4-dihydropyrimidin-1(2H)-yl}methyl)benzonitrile compounds with DPP-4 protein. Blue shows the compound structure of sitagliptin (control), and black shows the compound 2-({6-[(3R)-3-aminopiperidin-1-yl]-3-methyl-2,4-dioxo-3,4-dihydropyrimidin-1(2H)-yl}methyl)benzonitrile, while green is the DPP-4 protein.

Table 8. Interaction between compound and DPP-4 protein.

Compound	Binding energy (kJ/mol)	Interaction	Distance (A)	Binding category	Binding type
Loliolide	−201.4	:10:H16 - A:TYR547:OH	2.08654	Hydrogen bond	Conventional hydrogen bond
		A:TYR547 - :10:C9	5.2041	Hydrophobic	Pi-Alkyl
		A:TYR666 - :10:C9	3.94125	Hydrophobic	Pi-Alkyl
		A:HIS740 - :10:C7	3.98879	Hydrophobic	Pi-Alkyl
Moracin M	−308.2	:10:H9 - A:ASP739:OD1	1.77387	Hydrogen bond	Conventional hydrogen bond
		:10:H10 - A:GLU205:OE2	1.83875	Hydrogen bond	Conventional hydrogen bond
		A:ARG125:NH1 - :10	4.05942	Electrostatic	Pi-Cation
		A:ARG125:NH1 - :10	3.6655	Electrostatic	Pi-Cation
		A:HIS740:C,O;GLY741:N - :10	4.05044	Hydrophobic	Amide-Pi stacked
		A:HIS740:C,O;GLY741:N - :10	4.06935	Hydrophobic	Amide-Pi stacked
		:10 - A: ARG125	5.00327	Hydrophobic	Pi-Alkyl
		:10 - A: ARG125	4.1613	Hydrophobic	Pi-Alkyl
		A:LYS122:NZ - :10:H9	2.44879	Unfavorable	Unfavorable donor-donor
Formononetin	−261.8	A:ARG125:NH2 - :10:O2	2.47841	Hydrogen bond	Conventional hydrogen bond
		:10:H9 - A:ASP709:OD2	1.7697	Hydrogen bond	Conventional hydrogen bond
		A:HIS740:CD2 - :10:O2	2.74826	Hydrogen bond	Carbon hydrogen bond
		A:ARG125:NH1 - :10	4.2348	Electrostatic	Pi-Cation
		A:ARG125:NH1 - :10	4.73064	Electrostatic	Pi-Cation
		A:HIS740:CB - :10	3.85297	Hydrophobic	Pi-Sigma
		A:TRP629 - :10	5.16929	Hydrophobic	Pi-Pi T-shaped
		A:TRP629 - :10:C16	4.10504	Hydrophobic	Pi-Alkyl
		A:TRP629 - :10:C16	3.79111	Hydrophobic	Pi-Alkyl
		:10 - A: ARG125	4.74148	Hydrophobic	Pi-Alkyl
		:10 - A: ARG125	4.16958	Hydrophobic	Pi-Alkyl

(Continued)

Compound	Binding energy (kJ/mol)	Interaction	Distance (A)	Binding category	Binding type
Latifoline	−295.2	A:ARG125:NH2 - :10:O7	2.51919	Hydrogen bond	Conventional hydrogen bond
		A:TYR662:OH - :10:N1	2.58691	Hydrogen bond	Conventional hydrogen bond
		:10:H20 - A:GLU205:OE1	2.03586	Hydrogen bond	Conventional hydrogen bond
		:10:H1 - A:TYR662:OH	2.56552	Hydrogen bond	Carbon hydrogen bond
		:10:H2 - :10:O2	2.98769	Hydrogen bond	Carbon hydrogen bond
		:10:H11 - A:TYR547:OH	3.06717	Hydrogen bond	Carbon hydrogen bond
		:10:H13 - A:GLU205:O	1.71989	Hydrogen bond	Carbon hydrogen bond
		A:TYR547 - :10:C18	4.35117	Hydrophobic	Pi-Alkyl
		A:TRP629 - :10:C20	4.787	Hydrophobic	Pi-Alkyl
		A:TYR662 - :10	5.36216	Hydrophobic	Pi-Alkyl
		A:TYR662 - :10	5.47281	Hydrophobic	Pi-Alkyl
		A:TYR666 - :10	3.93524	Hydrophobic	Pi-Alkyl
		A:HIS740 - :10	4.48955	Hydrophobic	Pi-Alkyl
		A:HIS740 - :10:C20	4.37139	Hydrophobic	Pi-Alkyl
		A:GLU206:OE1 - :10:O4	2.88454	Unfavorable	Unfavorable acceptor-acceptor
Glycitein	−261.6	A:ARG125:NH2 - :10:O3	2.44764	Hydrogen bond	Conventional hydrogen bond
		:10:H8 - A:ASP709:OD2	2.07689	Hydrogen bond	Conventional hydrogen bond
		A:HIS740:CD2 - :10:O3	2.72543	Hydrogen bond	Carbon hydrogen bond
		:10:H10 - A:GLU205:OE2	2.1280	Hydrogen bond	Carbon hydrogen bond
		A:HIS740:CB - :10	3.76938	Hydrophobic	Pi-Sigma
		A:TRP629 - :10	5.10356	Hydrophobic	Pi-Pi T-shaped
		:10:C16 - A:ARG125	4.45695	Hydrophobic	Alkyl
		A:TRP124 - :10:C16	5.3498	Hydrophobic	Pi-Alkyl
		A:TRP201 - :10:C16	4.22045	Hydrophobic	Pi-Alkyl
		A:TRP201 - :10:C16	4.47248	Hydrophobic	Pi-Alkyl
		:10 - A: ARG125	4.94596	Hydrophobic	Pi-Alkyl
		:10 - A: ARG125	4.24752	Hydrophobic	Pi-Alkyl
Pectolinarigenin	−274.6	A:SER209:OG - :10:O2	3.12116	Hydrogen bond	Conventional hydrogen bond
		A:TYR631:N - :10:O6	3.00402	Hydrogen bond	Conventional hydrogen bond
		:10:H7 - A:SER209:OG	1.70339	Hydrogen bond	Conventional hydrogen bond
		:10:H8 - A:GLU206:O	1.98399	Hydrogen bond	Conventional hydrogen bond
		A:SER630:CB - :10:O6	3.63175	Hydrogen bond	Carbon hydrogen bond
		:10:H11 - :10:O4	2.65775	Hydrogen bond	Carbon hydrogen bond
		A:GLU206:OE1 - :10	3.49775	Electrostatic	Pi-Anion
		A:GLU206:OE1 - :10	3.38023	Electrostatic	Pi-Anion
		A:TYR666 - :10	4.05842	Hydrophobic	Pi-Pi stacked
		A:PHE357 - :10	4.95655	Hydrophobic	Pi-Pi T-shaped
		:10:C16 - A:ARG358	4.69835	Hydrophobic	Alkyl
		:10:C17 - A:VAL656	4.6022	Hydrophobic	Alkyl
		A:PHE357 - :10:C16	5.48682	Hydrophobic	Pi-Alkyl
		A:TYR631 - :10:C17	4.90607	Hydrophobic	Pi-Alkyl
		A:TRP659 - :10:C17	5.10768	Hydrophobic	Pi-Alkyl
		A:TYR662 - :10:C17	4.64083	Hydrophobic	Pi-Alkyl
		A:TYR666 - :10:C17	4.70685	Hydrophobic	Pi-Alkyl
		A:ARG669:NH2 - :10:H8	2.62431	Unfavorable	Unfavorable donor-donor

(Continued)

Compound	Binding energy (kJ/mol)	Interaction	Distance (A)	Binding category	Binding type
3-oxo-alpha-ionol	−213	:10:H20 - A:TRP629:O	1.84068	Hydrogen bond	Conventional hydrogen bond
		:10:H6 - A:TYR666	2.6142	Hydrophobic	Pi-Sigma
		A:TYR547 - :10:C6	5.25812	Hydrophobic	Pi-Alkyl
		A:TYR666 - :10:C6	4.23887	Hydrophobic	Pi-Alkyl
		A:HIS740 - :10:C10	3.86701	Hydrophobic	Pi-Alkyl
Sitagliptin	−330.8	A:ARG125:NH2 - :10:O1	2.887	Hydrogen bond	Conventional hydrogen bond
		A:TYR547:OH - :10:F4	3.397	Hydrogen bond: halogen	Conventional hydrogen bond: halogen (Fluorine)
		A:TYR631:N - :10:N3	2.63036	Hydrogen bond	Conventional hydrogen bond
		A:GLY632:N - :10:N5	3.27011	Hydrogen bond	Conventional hydrogen bond
		:10:H12 - A:GLU206:OE2	2.51282	Hydrogen bond	Conventional hydrogen bond
		:10:H12 - A:TYR662:OH	2.16614	Hydrogen bond	Conventional hydrogen bond
		:10:H2 - A:TYR547:OH	2.75542	Hydrogen bond	Carbon hydrogen bond
		:10:H2 - :10:F4	2.89965	Hydrogen bond	Carbon hydrogen bond
		:10:H3 - :10:F3	2.41648	Hydrogen bond	Carbon hydrogen bond
		:10:H5 - A:TYR547:OH	2.84051	Hydrogen bond	Carbon hydrogen bond
		:10:H9 - A:GLU205:OE1	3.04	Hydrogen bond	Carbon hydrogen bond
		A:GLU206:O - :10:F5	3.11723	Halogen	Halogen (Fluorine)
		A:GLU206:OE1 - :10:F5	3.61562	Halogen	Halogen (Fluorine)
		A:VAL546:O - :10:F1	3.1963	Halogen	Halogen (Fluorine)
		A:TRP629:O - :10:F1	3.02873	Halogen	Halogen (Fluorine)
		A:TRP629:O - :10:F2	3.46815	Halogen	Halogen (Fluorine)
		:10:N1 - :10:F4	3.55477	Halogen	Halogen (Fluorine)
		A:PHE357 - :10	4.05382	Hydrophobic	Pi-Pi Stacked
		:10 - A:TYR547	3.6064	Hydrophobic	Pi-Pi Stacked
		A:TYR547 - :10	4.24833	Hydrophobic	Pi-Alkyl
		A:TYR547 - :10:C11	4.17332	Hydrophobic	Pi-Alkyl
2-({6-[(3R)-3-aminopiperidin-1-yl] -3-methyl-2,4-dioxo-3,4-dihydropyridine-1(2H)-yl}methyl) benzonitrile	−291.2	A:TYR631:N - :10:O1	2.75598	Hydrogen bond	Conventional hydrogen bond
		:10:H18 - A:TYR662:OH	2.9153	Hydrogen bond	Conventional hydrogen bond
		A:SER630:CB - :10:O1	2.8953	Hydrogen bond	Carbon hydrogen bond
		:10:H2 - A:TRP629:O	2.68511	Hydrogen bond	Carbon hydrogen bond
		:10:H16 - A:GLU205:OE1	2.41845	Hydrogen bond	Carbon hydrogen bond
		:10:H23 - A:TYR547:OH	2.661	Hydrogen bond	Carbon hydrogen bond
		A:TYR547:OH - :10	3.25176	Hydrogen bond	Pi-Donor hydrogen bond
		A:TYR662:OH - :10	3.12186	Hydrogen bond	Pi-Donor hydrogen bond
		A:SER630:CB - :10	3.49264	Hydrophobic	Pi-Sigma
		A:TYR547 - :10	4.22248	Hydrophobic	Pi-Pi stacked
		A:TYR662 - :10	4.57868	Hydrophobic	Pi-Pi stacked
		A:TYR547 - :10:C2	3.41521	Hydrophobic	Pi-Alkyl
		A:TYR666 - :10	5.44585	Hydrophobic	Pi-Alkyl
		:10 - A: VAL711	5.13663	Hydrophobic	Pi-Alkyl

DISCUSSION

Extraction and DPP-4 inhibition activity of extracts

The extraction showed that the yield of methanol extract was higher from both leaves and stems. This makes it clear that the compounds contained in *P. canescens* are almost polar. The yield of hexane extract is the lowest because this plant contains fewer non-polar compounds. Several previous studies showed that the content of phytocomponents of this plant, among others, is alkaloids, flavonoids, tannins, phenols, terpenoids, and saponins [19,20]. Phytocomponents, such as alkaloids, flavonoids, tannins, phenols, terpenoids, and saponin, have been widely reported to have inhibitory activity against DPP-4. These phytocomponents or secondary metabolites are potential sources to be developed into new therapeutic agents [21–23].

In general, it can be seen that all extracts have inhibitory activity against DPP-4. Leaf extracts appear to be slightly superior to stem extracts. Ethyl acetate and methanol extract from the leaves showed better activity with percent inhibition of 70.09% ± 0.7233% and 59.69% ± 1.9394% (at 100 µg/ml) compared to other extracts, followed by ethyl acetate extract from the stem with percent inhibition of 58.20% ± 1.8244% (at 100 µg/ml).

Fractionation and DPP-4 inhibition activity of fractions

Fractionation is performed to separate parts of the extract, separating groups of compounds based on polarity differences depending on the eluent used. The presence of fractionation using a chromatographic column using a gradient system with a gradual increase in polarity is expected to be able to separate the active compound group (active fraction) from the less active compound group, leaving the most active part of the extract, which has better activity than the original extract. Several studies have shown that the most active fractions from column chromatography have better activity than the original extract [15,24,25]. However, it cannot be denied that column chromatography has a weakness when polar compounds are bound to a polar stationary phase, so recovery of polar compounds by this method will be poor [26,27].

The most active extracts, namely ethyl acetate and methanol extracts of *P. canescens* leaves, were fractionated to produce 12 and 10 fractions, respectively. In contrast to the activity of the original extract, the resulting fractions had better inhibition than the original extract. Several fractions (at 100 µg/ml) showed excellent activity, including the FPSEA3 fraction with a percent inhibition of 82.47% ± 0.5783%, the FPSM2 fraction with a percent inhibition of 88.28% ± 2.1204%, and the FPSM3 fraction with a percent inhibition of 85.49% ± 0.0854%. This could be due to the separation of the less active parts of the extract, resulting in fractions with better activity. Sitagliptin as a comparison standard showed better activity than the most active fraction (FPSM2) with a percent inhibition of 96.31% ± 0.1096% (at 100 µg/ml). This could be because sitagliptin is a single compound, while FPSM2 is a fraction that may contain even fewer active compounds. The isolation of FPSM2 in the future will be very promising to produce a DPP-4 inhibitor agent from *P. canescens* species.

Compound profiling of the most active fraction in DPP-4 inhibition

The strategy for identifying compounds with UPLC-QToF-MS/MS is based on peak analysis at a specific retention time and subsequent comparison with the database [28]. In various compound profiling analyses using UPLC-ESI-QToF-MS/MS, this method has been reported to be more sensitive and selective compared to other chromatographic methods [29]. Mass spectrometry analysis with QToF as a mass analyzer has the ability to detect various compounds. QToF, as a mass analyzer, can reveal mass information of compounds contained in the sample, making the structure identification of compounds more accurate and precise [30].

Seven peaks have been identified in the most active fraction (FPSM2), where the compounds detected are the flavonoids (glycitein, pectolinarigenin, and formononetin), an alkaloid (latifoline), phenol (moracin M), and terpenoids (3-oxo-α-ionol, loliolide). Compound profiling has never been done on this species before, and the compounds detected using UPLC-ESI-QToF-MS/MS are the first compounds identified in this species. Flavonoids contained in the most active fraction have a role in inhibiting the DPP-4 enzyme. Several studies have reported the potential of the flavonoids glycitein and formononetin in treating diabetes mellitus [31,32]. While glycitein has never been reported as a DPP-4 inhibitor, formononetin is reported to have inhibition against DPP-4 [33]. Sewidan *et al*. [34] reported the DPP-4 inhibitory activity of pectolinarigenin at a concentration of 100 mM with a percent inhibition of 34.7% ± 0.59%. Moracin M has been reported to have the potential for treating diabetes because of its ability to lower blood sugar through *in vivo* assays, inhibit enzymes associated with diabetes mellitus (α-Glucosidase, Protein Tyrosine Phosphatase 1B), and inhibit the formation of advanced glycation end products. Still, data on this compound related to DPP-4 inhibition has never been done [35–37]. Loliolide has been reported to have a role in antidiabetic activity [38,39], and its activity in inhibiting α-Amylase and α-Glucosidase has been reported [40]. Still, its inhibition of DPP-4 has never been reported before. The terpenoid compound 3-oxo-α-ionol and the alkaloid compound latifoline are reported for the first time to be contained in the active fraction of the DPP-4 inhibitor from the species *P. canescens*. Disclosure of these compounds shows the potential of this species in inhibiting the DPP-4, where compounds in the class of flavonoids, phenols, alkaloids, and terpenoids have been widely published as inhibitors of the DPP-4 [34,41–45].

Molecular docking

The control compounds used are two, sitagliptin as a comparator control, and the compound 2-({6-[(3R)-3-aminopiperidin-1-yl]-3-methyl-2,4-dioxo-3,4-dihydropyrimidin-1(2H)-yl}methyl)benzonitrile as an inhibitor control and docking validation control. Sitagliptin, as a control, showed the lowest binding energy, which was −330.8 kJ/mol. The bond energy of the complexes showed a range of bond energy values of −201.4–−330.8 kJ/mol, with the types of bonds detected in the complexes being hydrogen bonds, hydrophobic, and unfavorable bonds (Table 8). Based on the 3-D display of control compound complexes and DPP-4 protein, all compounds bind in the same region as the

inhibitor control (Fig. 2). The interaction of all compounds around the validation control compound indicates validated docking.

Arg125 residues with sitagliptin were also shown on the active side of moracin M, formononetin, latifoline, and glycitein compounds. Tyr547 residues were identified on the active side of loliolide, latifoline, 3-oxo-alpha-ionol, sitagliptin, and 2-({6-[(3R)-3-aminopiperidin-1-yl]-3-methyl-2,4-dioxo-3,4-dihydropyrimidin-1(2H)-yl}methyl)benzonitrile. Pectolinarigenin compound showed the same active side as the control, sitagliptin, and 2-({6-[(3R)-3-aminopiperidin-1-yl]-3-methyl-2,4-dioxo-3,4-dihydropyrimidin-1(2H)-yl}methyl) benzonitrile, namely at residue Tyr631. Residue Glu206, the active side of sitagliptin, was also detected as the active side of latifoline and pectolinarigenin. Residue Glu205 identified two control compounds, moracin M, latifoline, and glycetin. The compounds formononetin, latifoline, glycitein, and 3-oxo-alpha-ionol have an active side of Trp629, which was also identified in both control compounds (Figs. 3–5; Table 8).

CONCLUSION

Peronema canescens has been shown to have inhibitory activity against DPP-4, with the inhibitory activity of the most active fraction (FPSM2) reaching 88.28% ± 2.1204% at 100 µg/ml, suggesting that this plant has excellent potential to be developed as a drug for diabetes mellitus, especially as a DPP-4 inhibitor. Compound profiling has successfully revealed the compounds in FPSM2 as the most active fraction of *P. canescens,* including pectolinarigenin, glycitein, formononetin, latifoline, 3-oxo-alpha-ionol, moracin M, and loliolide. This study proves that the potential of *P. canescens* as an antidiabetic is limited to the inhibition activity of DPP-4. Therefore, further research is needed to confirm its various other antidiabetic mechanisms to reveal the complete mechanism of this plant as an antidiabetic.

ACKNOWLEDGMENT

The authors thank the Drug Development and Pharmacognosy-Phytochemistry Laboratory, Faculty of Pharmacy, Universitas Indonesia, and the Department of Pharmaceutical Chemistry, Faculty of Pharmacy, Universiti Malaya, for the support and research facilities provided. The author is also grateful to the Universitas Indonesia for the PUTI-Q2 grant that has been given.

AUTHOR CONTRIBUTIONS

The authors made significant contributions to the research conception and design, including to data collection or the analysis and interpretation of data; participated in the article drafting or the critical revision of the article about all intellectual content; consented to submission in the current journal; gave final approval for the version to be published; and agree to be responsible for all aspects of the work. The authors are eligible to be authors according to the guidelines of the International Committee of Medical Journal Editors (ICMJEs).

FINANCIAL SUPPORT

This project was supported by the PUTI-Q2 Grant (NKB-1172/UN2.RST/HKP.05.00/2022), Universitas Indonesia.

CONFLICT OF INTEREST

The authors report no financial or any other conflicts of interest in this work.

ETHICAL APPROVALS

This research does not involve human subjects or animals in the experiments.

DATA AVAILABILITY

All generated and analyzed research data are included in this article

PUBLISHER'S NOTE

This journal remains neutral with regard to jurisdictional claims in published institutional affiliation.

REFERENCES

1. Widyawati T, Yusoff NA, Bello I, Asmawi MZ, Ahmad M. Bioactivity-guided fractionation and identification of antidiabetic compound of *Syzygium polyanthum* (Wight.)'s leaf extract in streptozotocin-induced diabetic rat model. Molecules. 2022;27(20):6814.
2. Manalo RAM, Arollado EC, Heralde FM. Anti-hyperglycemic fraction from *Alternanthera sessilis* L. leaves gets elucidated following bioassay-guided isolation and mass spectrometry. Braz J Pharm Sci. 2023;59:e21283.
3. Ong KL, Stafford LK, McLaughlin SA, Boyko EJ, Vollset SE, Smith AE, *et al*. Global, regional, and national burden of diabetes from 1990 to 2021, with projections of prevalence to 2050: a systematic analysis for the Global Burden of Disease Study 2021. Lancet. 2023;402(10397):203–34.
4. Boyko EJ, Esztergalyos B, Gautam S, Helman B, Pinkepank M, Randi A, *et al*., editors. IDF diabetes atlas, Brussels, Belgium. 10th ed. IDF; 2021. vol. 64, 665–76 pp.
5. Galicia-Garcia U, Benito-Vicente A, Jebari S, Larrea-Sebal A, Siddiqi H, Uribe KB, *et al*. Pathophysiology of type 2 diabetes mellitus. Int J Mol Sci. 2020;21(17):1–34.
6. Zhou H, Liao J, Ou J, Lin J, Zheng J, Li Y, *et al*. Bioassay-guided isolation of Fenghuang Dancong tea constituents with α-glucosidase inhibition activities. Front Nutr. 2022;9(4):1050614.
7. Wu M, Yang Q, Wu Y, Ouyang J. Inhibitory effects of acorn (*Quercus variabilis* Blume) kernel-derived polyphenols on the activities of α-amylase, α-glucosidase, and dipeptidyl peptidase IV. Food Biosci [Internet]. 2021;43(April):101224. doi: https://doi.org/10.1016/j.fbio.2021.101224
8. Shaikh S, Lee E, Ahmad K, Ahmad S, Lim J, Choi I. A comprehensive review and perspective on natural sources as dipeptidyl peptidase-4 inhibitors for management of diabetes. Pharmaceuticals. 2021;14(591):1–18.
9. Chalichem NSS, Jupudi S, Yasam VR, Basavan D. Dipeptidyl peptidase-IV inhibitory action of Calebin A: an *in silico* and *in vitro* analysis. J Ayurveda Integr Med [Internet]. 2021;12(4):663–72. doi: https://doi.org/10.1016/j.jaim.2021.08.008
10. Kato E, Uenishi Y, Inagaki Y, Kurokawa M, Kawabata J. Isolation of rugosin A, B and related compounds as dipeptidyl peptidase-IV inhibitors from rose bud extract powder. Biosci Biotechnol Biochem [Internet]. 2016;80(11):2087–92. doi: http://dx.doi.org/10.1080/09168451.2016.1214533
11. Garber AJ, Handelsman Y, Grunberger G, Einhorn D, Abrahamson MJ, Barzilay JI, *et al*. Consensus statement by the American Association of clinical endocrinologists and American College of Endocrinology on the comprehensive type 2 diabetes management algorithm—2020 executive summary. Endocr Pract [Internet]. 2020;26(1):107–39. doi: https://doi.org/10.4158/CS-2019-0472
12. Jao CL, Hung CC, Tung YS, Lin PY, Chen MC, Hsu KC. The development of bioactive peptides from dietary proteins as a

dipeptidyl peptidase IV inhibitor for the management of type 2 diabetes. BioMedicine. 2015;5(3):9–15.
13. Cian RE, Nardo AE, Garzón AG, Añon MC, Drago SR. Identification and *in silico* study of a novel dipeptidyl peptidase IV inhibitory peptide derived from green seaweed *Ulva* spp. hydrolysates. Lwt. 2022;154:112738.
14. Latief M, Sari PM, Fatwa LT, Tarigan IL, Rupasinghe HPV. Antidiabetic activity of Sungkai (*Peronema canescens* Jack) leaves ethanol extract on the male mice induced alloxan monohydrate. Pharmacol Clin Pharm Res. 2021;6(2):64–74.
15. Triadisti N, Sauriasari R, Elya B. Antioxidant activity of fractions from *Garcinia hombroniana* Pierre leaves extracts. Pharmacogn J. 2018;10(4):682–5.
16. Cayman Chemical Company. DPP (IV) inhibitor screening assay Kit, Michigan, United States. Cayman Chemical Company; 2017.
17. Zhang Z, Wallace MB, Feng J, Stafford JA, Skene RJ, Shi L, *et al*. Design and synthesis of pyrimidinone and pyrimidinedione inhibitors of dipeptidyl peptidase IV. J Med Chem. 2011;54(2):510–24.
18. Bitencourt-Ferreira G, de Azevedo WF. Docking screens for drug discovery. 1st ed. In: de Azevedo WF, editor. Molegro Virtual Docker for Docking. Molegro Virtual Docker for Docking. New York, NY: Humana New York NY; 2019. vol. XVII, 286 p.
19. Maigoda T, Judiono J, Purkon DB, Haerussana ANEM, Mulyo GPE. Evaluation of *Peronema canescens* leaves extract: fourier transform infrared analysis, total phenolic and flavonoid content, antioxidant capacity, and radical scavenger activity. Open Access Maced J Med Sci. 2022;10(A):117–24.
20. Dillasamola D, Aldi Y, Wahyuni FS, Rita RS, Dachriyanus, Umar S, *et al*. Study of Sungkai (*Peronema canescens*, Jack) leaf extract activity as an immunostimulators with *in vivo* and *in vitro* methods. Pharmacogn J. 2021;13(6):1397–407.
21. Sarian MN, Ahmed QU, Mat So'Ad SZ, Alhassan AM, Murugesu S, Perumal V, *et al*. Antioxidant and antidiabetic effects of flavonoids: a structure-activity relationship based study. Biomed Res Int. 2017;2017:1–14.
22. Tran N, Pham B, Le L. Bioactive compounds in anti-diabetic plants : from herbal medicine to modern drug discovery. Biology (Basel). 2020;9(252):1–31.
23. Salleh NH, Zulkipli IN, Yasin HM, Jaafar F, Ahmad N, Amir W, *et al*. Systematic review of medicinal plants used for treatment of diabetes in human clinical trials : an ASEAN perspective. Hindawi—Evid Based Complement Altern Med. 2021;2021(Article ID 5570939):1–10.
24. Triadisti N, Rahayu S, Zamzani I. Metabolite profiling of *Ficus deltoidea*'s most active fraction as anti-*Candida albicans* using UPLC-QToF-MS/MS. J Young Pharm. 2021;13(1):58–62.
25. Mahayasih PGMW, Elya B, Hanafi M. Alpha-glucosidase inhibitory activity of *Garcinia lateriflora* Blume leaves. J Appl Pharm Sci. 2017;7(10):100–4.
26. Zhang S, Ma Y, Ma R, Wang Q, Dang J. Combination of medium- and high-pressure liquid chromatography for isolation of L-tryptophan (Q-marker) from *Medicago sativa* extract. Separations. 2022;9(9):1–11.
27. Nikoletta. A short notes on column chromatography. J Chromatogr Res [Internet]. 2021;4(1):1. Available from: https://www.scitechnol.com/peer-review/a-short-notes-on-column--chromatography-vUfW.php?article_id=18544
28. Wolfender JL, Marti G, Thomas A, Bertrand S. Current approaches and challenges for the metabolite profiling of complex natural extracts. J Chromatogr A. 2015;1382(February 2015):136–64.
29. Grata E, Guillarme D, Glauser G, Boccard J, Carrupt PA, Veuthey JL, *et al*. Metabolite profiling of plant extracts by ultra-high-pressure liquid chromatography at elevated temperature coupled to time-of-flight mass spectrometry. J Chromatogr A. 2009;1216(30):5660–8.
30. Li SL, Song JZ, Choi FFK, Qiao CF, Zhou Y, Han QB, *et al*. Chemical profiling of radix paeoniae evaluated by ultra-performance liquid chromatography/photo-diode-array/quadrupole time-of-flight mass spectrometry. J Pharm Biomed Anal. 2009;49(2):253–66.
31. Kuryłowicz A. The role of isoflavones in type 2 diabetes prevention and treatment—a narrative review. Int J Mol Sci. 2021;22(1):1–31.
32. Ahmed QU, Ali AHM, Mukhtar S, Alsharif MA, Parveen H, Sabere ASM, *et al*. Medicinal potential of isoflavonoids: polyphenols that may cure diabetes. Molecules. 2020;25(23):1–19.
33. Pan J, Zhang Q, Zhang C, Yang W, Liu H, Lv Z, *et al*. Inhibition of dipeptidyl peptidase-4 by flavonoids: structure–activity relationship, kinetics and interaction mechanism. Front Nutr. 2022;9(May):1–17.
34. Sewidan N, Khalaf RA, Mohammad H, Hammad W. *In-vitro* studies on selected Jordanian plants as dipeptidyl peptidase-IV inhibitors for management of diabetes mellitus. Iran J Pharm Res. 2020;19(4):95–102.
35. Kwon RH, Thaku N, Timalsina B, Park SE, Choi JS, Jung HA. Inhibition mechanism of components isolated from *Morus alba* branches on diabetes and diabetic complications via experimental and molecular docking analyses. Antioxidants. 2022;11(2):1–22.
36. Zhang M, Chen M, Zhang HQ, Sun S, Xia B, Wu FH. *In vivo* hypoglycemic effects of phenolics from the root bark of *Morus alba*. Fitoterapia [Internet]. 2009;80(8):475–7. doi: http://dx.doi.org/10.1016/j.fitote.2009.06.009
37. Jung M, Park M, Lee H, Kang YH, Kang E, Kim S. Antidiabetic agents from medicinal plants. Curr Med Chem. 2006;13(10):1203–18.
38. Grabarczyk M, Wińska K, Mączka W, Potaniec B, Anioł M. Loliolide–the most ubiquitous lactone. Folia Biol Oecol. 2015;11:1–8.
39. Song JH, Lee D, Lee SR, Yu JS, Jang TS, Nam JW, *et al*. Identification of bioactive heterocyclic compounds from mulberry and their protective effect against streptozotocin-induced apoptosis in INS-1 cells. Mol Med Rep. 2018;17(4):5982–7.
40. Thissera B, Visvanathan R, Khanfar MA, Qader MM, Hassan MHA, Hassan HM, *et al*. *Sesbania grandiflora* L. Poir leaves: a dietary supplement to alleviate type 2 diabetes through metabolic enzymes inhibition. S Afr J Bot [Internet]. 2020;130(February):282–99. doi: https://doi.org/10.1016/j.sajb.2020.01.011
41. Sharma D, Kumar S, Kumar S, Kumar D. DPP-IV inhibitors from natural sources: an alternative approach for treatment and management of diabetes. Indian J Nat Prod Resour. 2019;10(4):227–37.
42. Beidokhti MN, Lobbens ES, Rasoavaivo P, Staerk D, Jäger AK. Investigation of medicinal plants from Madagascar against DPP-IV linked to type 2 diabetes. S Afr J Bot [Internet]. 2018;115:113–9. doi: https://doi.org/10.1016/j.sajb.2018.01.018
43. Akhtar N, Jafri L, Green BD, Kalsoom S, Mirza B. A multi-mode bioactive agent isolated from *Ficus microcarpa* L. Fill. With therapeutic potential for type 2 diabetes mellitus. Front Pharmacol. 2018;9(NOV):1–12.
44. Gu L, Tian T, Xia L, Chou G, Wang Z. Rapid isolation of a dipeptidyl peptidase IV inhibitor from *Fritillaria cirrhosa* by thin-layer chromatography-bioautography and mass spectrometry-directed autopurification system. J Planar Chromatogr—Mod TLC. 2019;32(6):447–51.
45. Morikawa T, Ninomiya K, Akaki J, Kakihara N, Kuramoto H, Matsumoto Y, *et al*. Dipeptidyl peptidase-IV inhibitory activity of dimeric dihydrochalcone glycosides from flowers of *Helichrysum arenarium*. J Nat Med. 2015;69(4):494–506.

How to cite this article:
Elya B, Forestrania RC, Hashim NM, Triadisti N. Dipeptidyl peptidase-4 inhibition of *Peronema canescens* Jack leaves and stems: Bioassay-guided fractionation, compound profiling by LC-MS/MS, and interaction mechanism. J Appl Pharm Sci. 2024.
http://doi.org/10.7324/JAPS.2024.161007